Recent progress in coincidence studies on ion desorption induced by core excitation

2006 J. Phys.: Condens. Matter 18 S1389

(http://iopscience.iop.org/0953-8984/18/30/S03)

INSTITUTE OF PHYSICS PUBLISHING JOURNAL OF PHYSICS: CONDENSED MATTER

J. Phys.: Condens. Matter **18** (2006) S1389–S1408 doi:10.1088/0953-8984/18/30/S03

Recent progress in coincidence studies on ion desorption induced by core excitation

Eiichi Kobayashi[1,2], Kazuhiko Mase[1,3], Akira Nambu[1,8], Junya Seo[4], Shinichiro Tanaka[5], Takuhiro Kakiuchi[6], Koji K Okudaira[7], Shin-ichi Nagaoka[6] and Masatoshi Tanaka[4]

[1] Institute of Materials Structure Science, KEK, Tsukuba 305-0801, Japan
[2] Inoue Foundation for Science, Shibuya-ku 150-0036, Japan
[3] PRESTO, Japan Science and Technology Agency, Kawaguchi 332-0012, Japan
[4] Faculty of Engineering, Yokohama National University, Yokohama 240-8501, Japan
[5] The Institute of Scientific and Industrial Research, Osaka University, Ibaraki 567-0047, Japan
[6] Department of Chemistry, Faculty of Science, Ehime University, Matsuyama 790-8577, Japan
[7] Faculty of Engineering, Chiba University, Chiba 263-8522, Japan

E-mail: eiichik@post.kek.jp

Received 30 November 2005, in final form 6 February 2006
Published 14 July 2006
Online at stacks.iop.org/JPhysCM/18/S1389

Abstract

This paper reports on recent studies of photostimulated ion desorption (PSID) using electron ion coincidence (EICO) spectroscopy combined with synchrotron radiation. H^+ desorption from H_2O dissociatively adsorbed on Si(111) and SiO_2/Si(111) surfaces (H_2O/Si(111) and H_2O/SiO_2/Si(111)) was studied for Si L-edge excitation. The Si 2p–H^+ photoelectron photoion coincidence (PEPICO) and Si 2p photoelectron spectra of H_2O/Si(111) and H_2O/SiO_2/Si(111) show that H^+ desorption probability increases as the number of positive charges at the Si site increases. The H^+ desorption probability per Si 2p ionization for the Si^{4+} site was estimated and found to be 5–7×10^{-5}. We proposed a mechanism that H^+ desorption is induced by Si 2p photoionization accompanied by a Si LVVV double-Auger transition. This article also reviews recent EICO work on site-specific ion desorption of 1,1,1-trifluoro-2-propanol-d_1 ($CF_3CD(OH)CH_3$) adsorbed on Si(100) surfaces, and on the mechanisms of PSID of poly(tetrafluoroethylene) (PTFE) and TiO_2(110). Clear site-specific ion desorption was observed for the C 1s core excitation of a $CF_3CD(OH)CH_3$ sub-monolayer on Si(100). A spectator-Auger-stimulated ion-desorption mechanism was proposed for F^+ desorption induced by a transition from F 1s to σ(C–F)* of PTFE. O^+ desorption induced by O 1s excitation of TiO_2(110) was attributed mainly to three-hole final states resulting from multi-electron excitation/decay. For O^+ desorption induced by Ti core excitation of TiO_2(110), on the other hand, charge transfer from an O 2p orbital to a Ti 3d orbital, instead of the interatomic Auger transition, was proposed to

[8] Present address: Chemistry Department, Brookhaven National Laboratory, Upton, NY 11973-500, USA.

be responsible for the desorption. These investigations demonstrate that EICO spectroscopy combined with synchrotron radiation is a useful tool for studying PSID.

(Some figures in this article are in colour only in the electronic version)

1. Introduction

Since the concept of desorption induced by electronic transitions (DIET) was put forward by Isikawa [1, 2], Ohta [3], Menzel and Gomer [4], and Redhead [5], DIET has developed into an active field in surface science [6, 7]. Recently, desorption induced by transitions from core levels became one of the forefront themes of this field [8–11]. Synchrotron radiation is an ideal light source to study DIET, because state-selective excitations are accessible owing to the tunability and high polarization of the radiation, and because the secondary processes due to secondary electrons are drastically reduced. The mechanism of DIET has been discussed mainly based on measurements of the desorption yield as a function of the excitation energy (desorption yield spectroscopy) so far. Desorption yield spectroscopy presents information on the correlation between the initial transitions and the desorption processes. Secondary processes, such as x-ray induced electron-stimulated desorption (XESD) [12], however, often smear information on the correlation. Furthermore, information on intermediate processes, such as Auger decays, cannot be obtained by desorption yield spectroscopy. For study of Auger-stimulated ion desorption (ASID) [13–16], Auger photoelectron coincidence spectroscopy (APECS) [17, 18], photoelectron photoion coincidence (PEPICO) spectroscopy [10, 18, 19], and Auger electron photoion coincidence (AEPICO) spectroscopy [10, 18, 20, 21] are ideal approaches, because they provide information on the correlation among the initial transitions, the intermediate Auger transitions, and the ion desorption, as shown in figure 1. The ion desorption using electron ion coincidence (EICO) spectroscopy so far has been described in detail in previous overviews [10, 22, 23].

In this paper we describe the present status of the electron ion coincidence apparatus (section 2), a H^+ desorption study of water dissociatively adsorbed on Si(111) and SiO_2/Si(111) surfaces by using PEPICO spectroscopy (section 3), a site-specific ion desorption study of 1,1,1-trifluoro-2-propanol-d_1 [$CF_3CD(OH)CH_3$] dissociatively adsorbed on Si(100) surfaces (section 4), ion desorption induced by core excitation of poly(tetrafluoroethylene) (section 5), and ion desorption induced by core excitation of TiO_2(110) (section 6). Finally we summarize our conclusions and the future prospects of EICO spectroscopy (section 7).

2. Apparatus for electron ion coincidence spectroscopy

In 1997, one of the authors (KM) and his collaborators developed an electron ion coincidence (EICO) apparatus combined with synchrotron radiation [20]. Since then, KM and his collaborators have remodelled the coincidence analyser several times [10]. Figure 2 shows a schematic diagram of the latest analyser for electron ion coincidence spectroscopy.

The latest EICO apparatus consists of a coaxially symmetric mirror electron energy analyser (coASMA) with a diameter of 140 mm, a time-of-flight ion mass spectrometer (TOF-MS) with a diameter of 26 mm, a magnetic shield, an xyz and tilt stage, and a conflat flange with a diameter of 203 mm. The original coaxially symmetric mirror analyser was developed by Siegbahn *et al* in 1997 [24]. We have improved their analyser and developed a modified one,

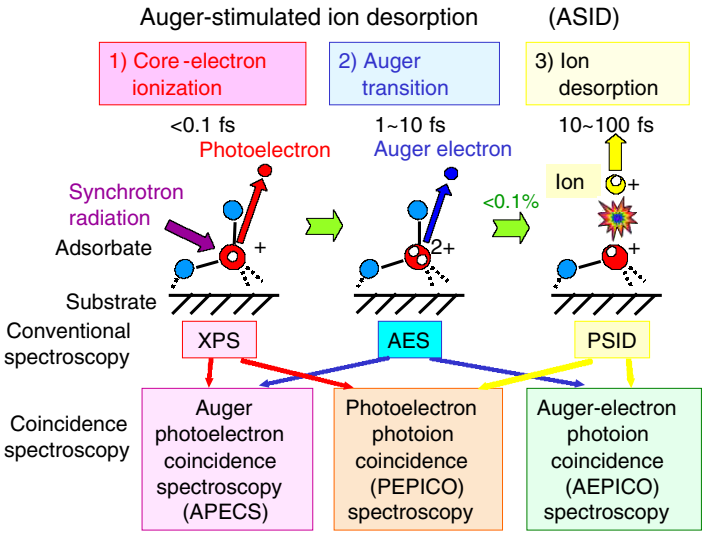

Figure 1. Schematic diagram of an Auger-stimulated ion desorption (ASID) mechanism; that is, (1) core-electron ionization, (2) a normal Auger transition leading to a $(\text{valence})^{-2}$ state, and (3) ion desorption along the repulsive potential energy surface of the $(\text{valence})^{-2}$ state. APECS, PEPICO, and AEPICO spectroscopy are ideal approaches for an ASID study, because they provide information on the correlation among the initial ionizations, the intermediate Auger transitions, and the final ion desorption.

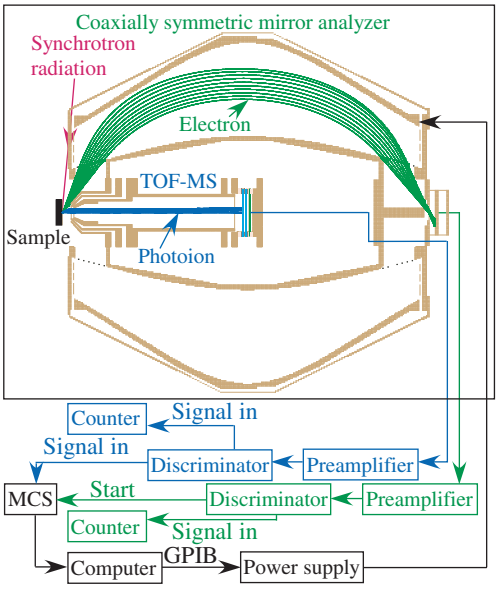

Figure 2. Schematic diagram of the EICO apparatus combined with synchrotron radiation.

which consists of an inner electrode, an outer electrode, three sets of compensation electrodes, a pinhole, microchannel plates (MCPs) and a magnetic shield [25]. The TOF-MS consists of a shield for the electric field, an ion-extraction electrode, a drift tube and MCPs. The TOF-MS is assembled in the coASMA coaxially and confocally. The electrons and ions are detected by

the coASMA and TOF-MS, respectively. The trajectories of electrons and ions simulated with SIMION 3D version 7.0 (http://www.simion.com/) are also shown in figure 2. The ion signals are measured with a multichannel scaler (MCS) as a function of the TOF difference between the electron and ion signals. An ion desorbed simultaneously with a trigger electron gives a coincidence signal at a specific TOF difference. The integrated coincidence signals plotted against the electron kinetic energy give an EICO spectrum.

3. H^+ desorption from H_2O dissociatively adsorbed on Si(111) and SiO_2/Si(111) surfaces

Studying water dissociatively adsorbed on Si(111) and SiO_2/Si(111) surfaces (H_2O/S(111) and H_2O/SiO_2/Si(111)) is important not only in fundamental science, but also in industrial fields, such as wet etching of semiconductor devices and catalysis. Since photostimulated ion desorption (PSID) is sensitive to surface hydrogen, H^+ desorption induced by the Si 2p excitations of H_2O/Si(111) and H_2O/SiO_2/Si(111) is an attractive topic. Conventional desorption yield spectroscopy is not adequate to investigate these samples for Si L-edge excitation, because XESD [12] due to abundant secondary electrons from the Si substrate smears any desorption induced by direct Si 2p excitations. Photoelectron photoion coincidence (PEPICO) spectroscopy is an alternative and useful approach, because the ion yield derived from XESD is suppressed, because core-level photoelectron spectroscopy can distinguish two atomic sites whose chemical shifts are different, and because the desorption probability per core-electron ionization can be obtained quantitatively [26].

3.1. H^+ desorption from H_2O dissociatively adsorbed on Si(111) for the Si L-edge excitation

H_2O is dissociatively adsorbed on a Si(111) surface (H_2O/Si(111)) at room temperature, forming Si–OH and Si–H surface species. Previously, the photostimulated ion desorption (PSID) of H^+ from H_2O dissociatively adsorbed on Si(100) (H_2O/Si(100)) for the O K-edge excitation was studied [27, 28]. Tanaka *et al* investigated the mechanism of H^+ desorption from H_2O/Si(100) using PEPICO and Auger electron photoion coincidence (AEPICO) spectroscopy, and reported that three-valence-hole states created through O 1s ionization accompanied by double Auger or through shake-up/off O 1s ionization accompanied by Auger are responsible for H^+ desorption [28].

In this section, we focus on H^+ desorption from H_2O/Si(111) for the Si L-edge excitation. Photoelectron and PEPICO experiments were carried out at the Photon Factory (PF) 11D. Partial electron yield (PEY) and total ion yield (TIY) measurements were performed at PF-8A, which is equipped with a Zeiss SX-700. The angle of the incident p-polarized synchrotron radiation was 84° from the surface normal. H_2O/Si(111) was prepared by flashing Si(111) by direct-current heating under an ultrahigh vacuum, and subsequent exposure to H_2O gas of about 1000 L at room temperature.

Figure 3 shows PEY and TIY spectra for H_2O/Si(111) at room temperature for the Si L-edge excitation. The TIY increases by about 10%, while the PEY is enhanced by about 170% at the Si L-edge. Besides, the shoulder and the peak positions as well as the shape of TIY resemble those of the PEY. These results indicate that XESD dominates over desorption directly induced by Si 2p excitations. Therefore, it is difficult to discuss the correlation between the initial electronic transition and ion desorption based on the PEY and TIY spectra.

Figure 4 shows Si 2p–H^+ PEPICO and Si 2p photoelectron spectra of a H_2O/Si(111) surface at $h\nu = 130$ eV. The time of measurement was 3900 s for each PEPICO datum. The H^+ PEPICO peak was observed at a relative binding energy of +1.5 eV, corresponding to the Si^+ and Si^{2+} sites. This result indicates that H^+ desorption takes place at the Si^+ and Si^{2+} sites.

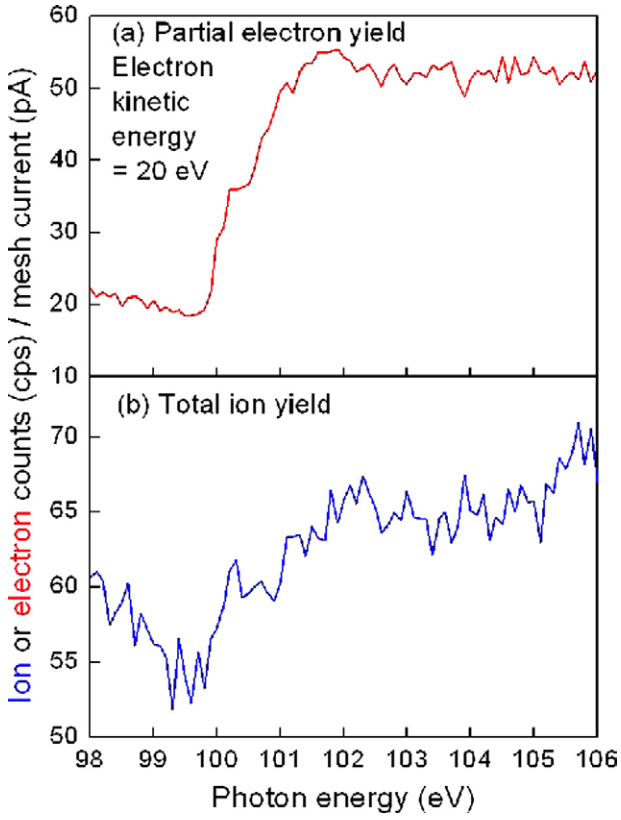

Figure 3. (a) Partial electron yield (PEY) spectrum for an electron kinetic energy of 20 eV and (b) total ion yield (TIY) spectrum of a Si(111) surface exposed to H_2O gas of about 1000 L at room temperature.

We estimated the H^+ desorption probability per Si 2p ionization (P_D), as shown in figure 5, by the following equation:

$$P_D = \frac{C_{PEPICO}}{C_{PE} \times R_{Si\ 2p} \times E_{PI}},$$

where C_{PEPICO} and C_{PE} denote Si 2p–H^+ PEPICO, and the photoelectron counts measured with the EICO analyser simultaneously at a specific photoelectron kinetic energy. The latter is the same as the number of the trigger for the MCS during the coincidence measurement (see figure 2). $R_{Si\ 2p}$ is the ratio of the Si 2p photoelectron counts to the electron counts at a specific electron kinetic energy. E_{PI} is the photoion detection efficiency of the TOF-MS, given by the following equation:

$$E_{PI} = (T_{Mesh})^3 \times E_{MCP},$$

where T_{Mesh} is the transmittance of one mesh in the TOF-MS ($T_{Mesh} = 0.77$) and E_{MCP} is the photoion detection efficiency of the MCPs ($E_{MCP} = 0.6$). The values of P_D were estimated to be $<4 \times 10^{-6}$, $5–7 \times 10^{-6}$ and $2–4 \times 10^{-5}$ for the Si^0, Si^+ and Si^{2+} sites, respectively (figure 5). We assigned the Si^+ and Si^{2+} sites responsible for the H^+ desorption to the Si–OH and Si(O)–OH sites, respectively (figure 6).

We also carried out Si 2p–H^+ PEPICO measurements of Si(111) exposed to H_2O gas of about 5 L, on which Si–OH and Si–H sites exist. The H^+ PEPICO signal, however, was below

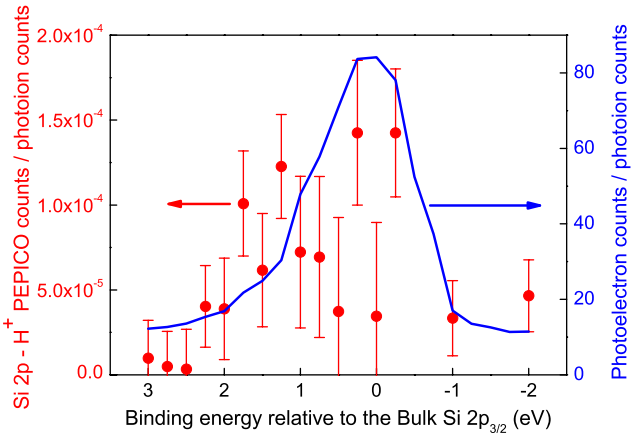

Figure 4. Si 2p–H^+ PEPICO (filled circles) and Si 2p photoelectron (solid line) spectra of a H_2O/Si(111) surface at $h\nu = 130$ eV. Both spectra are normalized by the ion counts simultaneously measured with the EICO analyser.

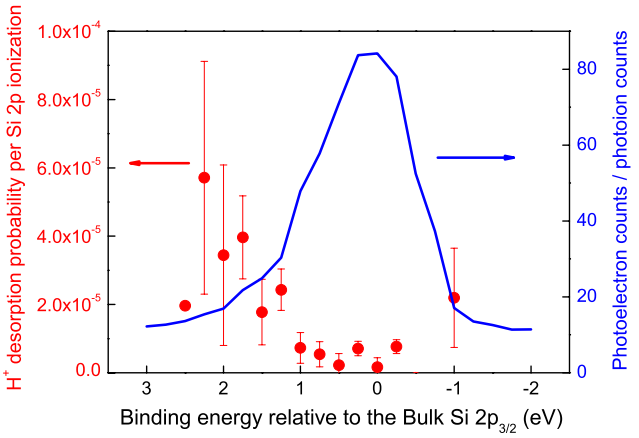

Figure 5. H^+ desorption probability per Si 2p ionization (filled circles) and Si 2p photoelectron spectrum (solid line) of a H_2O/Si(111) surface.

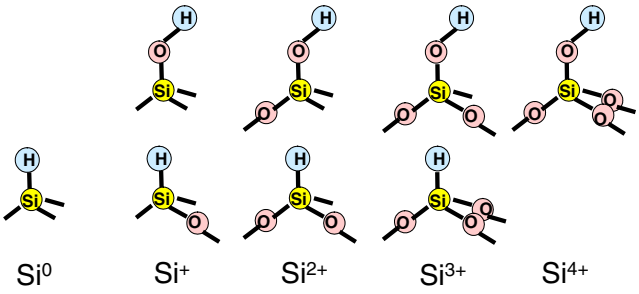

Figure 6. Schematic diagrams of the surface Si sites with a hydrogen.

the detection limit of our apparatus ($P_D < 4 \times 10^{-6}$). The results show that H^+ desorption probability is quite small at the Si–OH and Si–H sites.

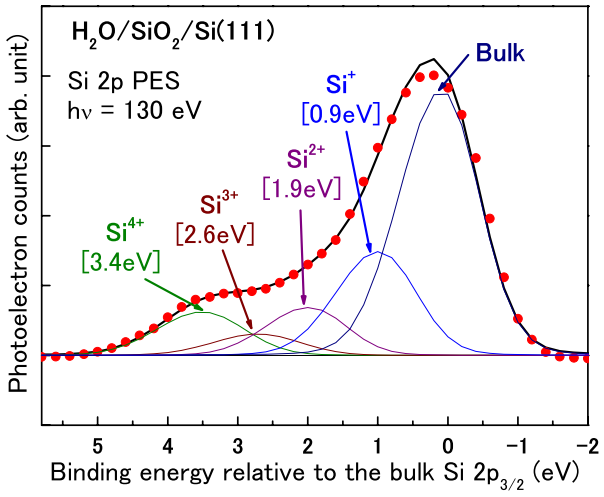

Figure 7. Si 2p photoelectron spectrum of $H_2O/SiO_2/Si(111)$ at room temperature. The photon energy was 130 eV. The raw data are shown as filled circles and suboxide components (Si^+, Si^{2+}, Si^{3+} and Si^{4+}) are shown as solid lines. The sum of all components is shown as the thick solid line.

3.2. H^+ desorption from H_2O dissociatively adsorbed on $SiO_2/Si(111)$ for the Si L-edge excitation

We next describe a study of H^+ desorption from H_2O dissociatively adsorbed on SiO_2 on Si(111) ($H_2O/SiO_2/Si(111)$) for Si L-edge excitation. $H_2O/SiO_2/Si(111)$ was prepared by flashing Si(111) by direct-current heating under an ultrahigh vacuum and subsequent exposure to 100 L of oxygen (O_2) mixed with H_2O of 2% at room temperature. Figure 7 shows a Si 2p photoelectron spectrum (PES) at $h\nu = 130$ eV. Si 2p peaks with a chemical shift of 0–4 eV from the peak position of the bulk Si $2p_{3/2}$ were observed. In a Si 2p PES study of $SiO_2/Si(111)$ using synchrotron radiation, Hollinger and Himpsel assigned the Si 2p peaks appearing with chemical shifts of 0.9, 1.9, 2.6 and 3.4 eV from the bulk Si 2p to the Si^+, Si^{2+}, Si^{3+} and Si^{4+} sites, respectively [29]. The curve fitting using Voigt functions based on the assignments is also shown in figure 7.

Figure 8 shows the Si 2p–H^+ PEPICO and Si 2p photoelectron spectra of $H_2O/SiO_2/Si(111)$ at room temperature. The time of measurement was 11 400 s for each PEPICO datum. A clear H^+ coincidence signal was observed at a chemical shift of 3 eV relative to the bulk Si $2p_{3/2}$, which corresponds to the Si^{3+} and Si^{4+} sites. However, the H^+ PEPICO signal was small for the photoelectron peak at the Si^0 site. This result shows that H^+ desorption is induced mainly by the photoionization of Si 2p at the sub-oxide components.

We estimated the H^+ desorption probability per Si 2p ionization at the Si^0, Si^+, Si^{2+}, Si^{3+} and Si^{4+} sites to be $<5 \times 10^{-6}$, $1–2 \times 10^{-5}$, $1–2 \times 10^{-5}$, $3–4 \times 10^{-5}$ and $5–7 \times 10^{-5}$, respectively, as shown in figure 9. The H^+ desorption probability per Si 2p ionization at the Si^{4+} site corresponding to SiO_2 (see figure 6) was the largest of all. In PEPICO and AEPICO studies of $H_2O/Si(100)$ for O K-edge excitation, Tanaka *et al* concluded that three-valence-hole states are responsible for the H^+ desorption [28]. Therefore, we propose the following H^+ desorption mechanism in the present case, as shown in figure 10: that is, (1) the formation of a core hole by a Si 2p photoelectron emission, (2) the formation of a three-valence-hole state by a Si LVVV double Auger transition, and (3) H^+ desorption induced by Coulomb repulsion among the three holes, and by electrons missing from O–H bonding orbitals.

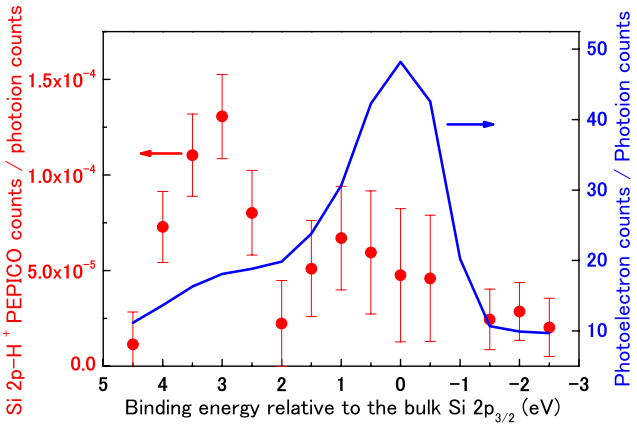

Figure 8. Si 2p–H^+ PEPICO data (filled circles) and Si 2p photoelectron spectrum (solid line) of a $H/SiO_2/Si(111)$ surface at $h\nu = 130$ eV. Both spectra are normalized by the photoion counts simultaneously measured with the EICO analyser.

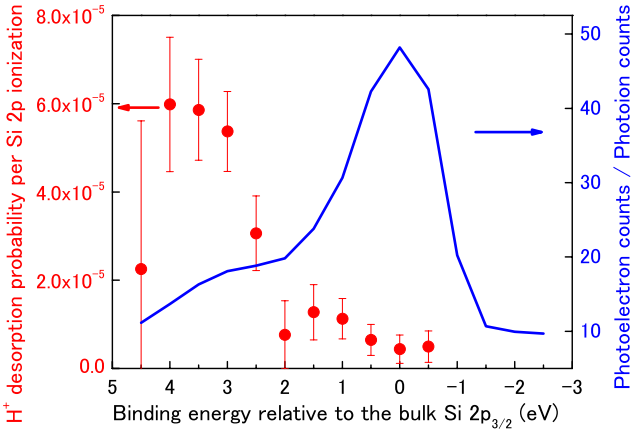

Figure 9. H^+ desorption probability (filled circles) and Si 2p photoelectron spectrum (solid line) of $H/SiO_2/Si(111)$.

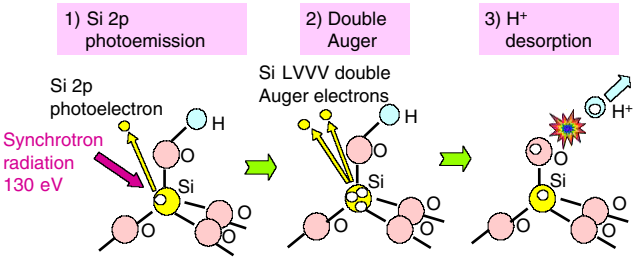

Figure 10. Proposed H^+ desorption mechanism induced by Si 2p photoelectron emission at the Si^{4+} site of $H/SiO_2/Si(111)$.

The H^+ desorption probability increases as the number of positive charges at the Si site increases. We attributed the increase to an increase in the lifetime of the three-valence-hole

state responsible for the H^+ desorption. The lifetime is expected to be longer when the number of positive charges at the Si site increases, because the electron transfer from the neighbouring Si is suppressed as the number of neighbouring O increases. The H^+ desorption probability per Si 2p ionization at the Si^{2+} site of $H_2O/SiO_2/Si(111)$ was smaller than that of $H_2O/Si(111)$. The difference may be attributed to the presence of the Si^{2+} sites in the interface between SiO_2 and Si(111). The present study demonstrates that the Si 2p–H^+ PEPICO measurement is a promising tool for analysing the OH species on Si surfaces.

4. Site-specific ion desorption induced by core excitation of $CF_3CD(OH)CH_3$ adsorbed on Si(100)

One of the exciting findings in photoionization dynamics caused by core excitation is site-specific fragmentation. It induces selective bond dissociation around a core-excited atomic site in a molecule including multiple non-equivalent atoms that have the same atomic number, but the chemical environments around which are different from one another [9, 21, 30–36]. Site-specific fragmentation is potentially useful for controlling chemical reactions through selective bond dissociation, and also offers possibilities of analysing the structures and properties of molecules, molecular assemblies and nanoscale devices by controlling matter at the level of individual atoms.

Site-specific fragmentation has been studied mainly in the vapour phase [30–32, 34, 36] and in the condensed phase [21, 33], but only a few studies have been devoted to that for monolayer adsorbates on surfaces [9, 35]. In the monolayer regime, competition between the intramolecular electronic relaxation and the electron–substrate interaction may make the site-specific fragmentation complex. Site-specificity may also be influenced by the geometry of adsorption. Furthermore, information about the effect of the substrate in the monolayer regime will provide a foundation to study controversial subjects (e.g., catalysis, corrosion and nanoscience on surfaces). Accordingly, there are good reasons for studying the site-specific fragmentation of a simple organic molecule that has a few non-equivalent carbon sites with different chemical environments, and is easily adsorbed on a surface. For such an investigation, the electron ion coincidence (EICO) technique, which is the main subject of this paper, is very suitable.

In this section, we describe a recent study on the site-specific fragmentation caused by C 1s core-level photoionization of 1,1,1-trifluoro-2-propanol-d_1 [$CF_3CD(OH)CH_3$, TFIP-d_1] [37] adsorbed on a Si(100) surface. This molecule is expected to show the site-specific fragmentation because the chemical environments of the individual carbon sites are very different from one another. TFIP-d_1 seems to be dissociatively adsorbed like $(CF_3)(CH_3)CDO$–Si(100) as shown in figure 11.

Figure 12(a) shows the PES of TFIP-d_1 sub-monolayer on a Si(100) surface at room temperature. The spectrum has three peaks in the range of C 1s photoelectron emission. These peaks are assigned, in ascending order of the binding energy, to 1s electron emissions from the central carbon atom (C[O]), from the carbon atom bonded to three hydrogen atoms (C[H]) and from the carbon atom bonded to three fluorine atoms (C[F]). The chemical shifts (binding energies) at the three carbon sites are different from one another.

Figures 12(b)–(d) show the PEPICO TOF spectra obtained with the emission of the C[O] 1s, C[H] 1s and C[F] 1s electrons, respectively. Site-specific fragmentation is clearly revealed in the PEPICO TOF spectra of a TFIP-d_1 sub-monolayer at room temperature. F^+ ions were abundantly desorbed coincidentally with the C[F] 1s photoelectron emission (figure 12(d)), but were negligible in the PEPICO TOF spectra for the C[O] and C[H] 1s photoelectron emissions (figures 12(b) and (c)). The intensity of H^+ for the C[F] 1s photoelectron emission seems to be

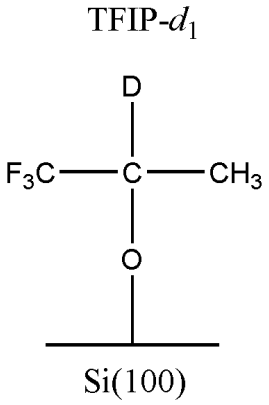

Figure 11. Structure of TFIP-d_1 chemisorbed on a Si(100) surface.

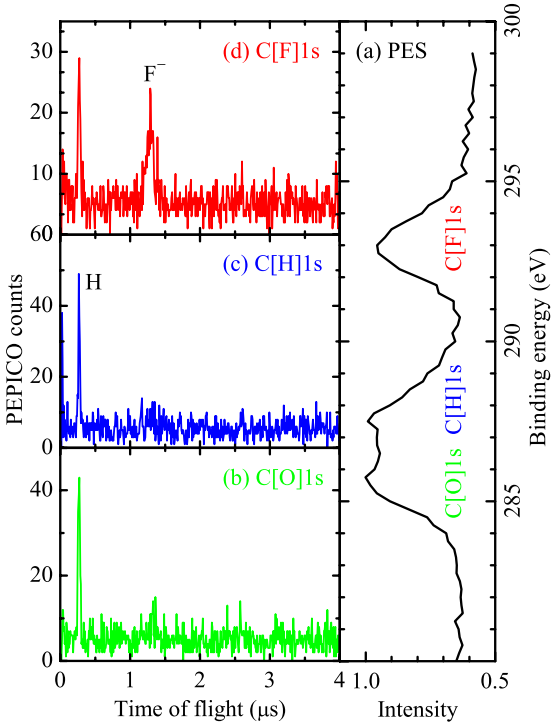

Figure 12. (a) PES in the region of C 1s electron emission of a TFIP-d_1 sub-monolayer chemisorbed on a Si(100) surface at room temperature. The unit of the intensity is arbitrary. (b) PEPICO TOF spectrum obtained with (b) the C[O] 1s, (c) C[H] 1s and (d) C[F] 1s electron emissions.

less than that for the C[H] 1s and C[O] 1s photoelectron emissions. The production of H^+ by the C[H] 1s photoionization and of F^+ by the C[F] 1s photoionization shows that site-specific fragmentation occurs at the carbon atom where photoionization has taken place.

H^+ ions are coincidentally desorbed in all of the spectra. H^+ is expected to have a high yield (because of its low mass and fast exit velocity), causing reneutralization to be less effective

compared with any heavier ion. Note that H^+ ions are also desorbed coincidentally with the C[O] 1s and C[F] 1s photoelectron emissions. If fragmentation occurs selectively at the core-ionized carbon atom, H^+ ions should be desorbed only by the C[H] 1s photoionization. The reason for the absence of site-specificity for H^+ is thought to be that H^+ has a high yield and the three carbon sites are close to each other. In fact, we previously showed that the site-specificity in $X_3Si(CH_2)_nSi(CH_3)_3$ (X = F or Cl, n = 0–2) decreases with decreasing distance between the two silicon sites [38]. As in $X_3Si(CH_2)_nSi(CH_3)_3$, effective electron migration among the three carbon sites is probably responsible for the absence of site-specificity for H^+.

In the PEPICO TOF spectrum for the C[O] 1s photoelectron emission (figure 12(b)), the intensities of PEPICO TOF signals of ion species other than H^+ are low, and the spectrum is similar to that for the C[H] 1s photoelectron emission that leads to H^+ production through fragmentation specific to the C[H] site. The similarity is likely due to effective substrate-to-C[O] electron transfer; that is, although some heavy ions specific to the C[O] site (for example, CH_3^+ or CF_3^+) may be produced by selective dissociation at the core-ionized C[O] atom, they are, owing to their relatively slow movement, reneutralized effectively by electron transfer through the Si–O–C bond, and are negligible in the PEPICO TOF spectrum (figure 12(b)). If the reneutralized species were detected, the fragmentation specific to the C[O] site would be clearly revealed. The specificity to the C[O] site must be enhanced by electron transfer from the substrate to the C[O] site, but neutral species are not easily detected.

Furthermore, as in 2,2,2-trifluoroethanol (CF_3CH_2OH) adsorbed on Si(100) [39], the bulky CF_3 group may shield the C[O] site from the TOF tube. Even if the photoelectron could escape from the C[O] site, the bulky CF_3 group might keep the coincidentally desorbed ions from reaching the TOF tube. The ions released from the C[O] site would thus be pushed back toward the substrate and neutralized. The bulky CF_3 group may thus prevent the disclosure of fragmentation specific to the C[O] site.

5. Ion desorption induced by core excitation of poly(tetrafluoroethylene)

Poly(tetrafluoroethylene) (PTFE, $(–CF_2–)_n$) is a candidate material in many applications, such as making microparts for bioscience and medical application because of its superior thermal and chemical stability. However, the application of micromachining technology to PTFE was difficult since there are few solvents to dissolve this polymer and heating over its melting point does not result in enough fluidity for modelling. Recently, the degradation of PTFE by irradiation of a vacuum ultraviolet pulsed laser, x-rays, and low-energy electrons has been reported [40–42]. The analysis of ion desorption induced by core excitation is one of the useful methods to clarify the relationship between the photodegradation mechanism and the electronic configuration of excited states. Especially, site-selective photofragmentation of polymer films provides a new possibility to synthesize new materials for practical use. The photostimulated ion desorption (PSID) of poly(methylmethacrylate) (PMMA) film has been reported, where desorbed ions were highly dependent on the photon energy near the carbon and oxygen K absorption edges [33]. It was observed that the photodegradation process of PMMA depends on the nature of the electronic state created in the polymer film by core excitation. Recently, for fluorinated compounds, such as poly(tetrafluoroethylene) (PTFE) and fluorinated copper phthalocyanine ($F_{16}CuPc$), selective F^+ desorption has been found to occur by the irradiation of photons corresponding to the transition from F 1s to σ(C–F)* [43, 44]. The results demonstrate the possibility that chemical bonds in molecular systems can be broken efficiently using monochromatic synchrotron radiation. To achieve more efficient bond scission, one needs to clarify the mechanism of ion desorption induced by core excitation.

In this section, we describe the mechanism of ion desorption from PTFE for the F K-edge excitation. In particular, we focus on the process of the effective C–F bond scission

(F^+ desorption) by the irradiation of photons corresponding to the transition from F 1s to σ(C–F)* (σ(C–F)* $\leftarrow$ F 1s). It is well known that following a resonant transition into an unoccupied level a spectator-Auger transition occurs. This process results in a two-hole–one-electron (2h1e) state, in which two holes are produced in valence orbitals and one electron is excited to an antibonding valence orbital. In order to clarify the mechanism of ion desorption following core excitation, F^+ desorption from PTFE was investigated for F K-edge excitation using Auger electron photoion coincidence (AEPICO) spectroscopy. AEPICO spectroscopy has become one of the most powerful tools because it can be used to measure ion desorption yields for selected Auger transitions [10, 22, 23].

PTFE was supplied by Central Glass (Cefralrub TFO-I). It is a mixture of n-C_nF_{2n+2} of $n = 100$–400, with the maximum at $n = 170$. PTFE thin films with a thickness of about 100 Å were evaporated on a Cu plate. Experiments were performed at PF-8A and 13C. AEPICO spectra were measured by using an EICO apparatus, composed of a coaxially symmetric mirror electron energy analyser [25] and a polar-angle-resolved compact time-of-flight (TOF) ion mass spectrometer with four concentric anodes [45]. The total electron yield (TEY) and total ion yield (TIY) as well as the Auger and AEPICO spectra were observed at the incidence angle of the p-polarized radiation of 84° (grazing incidence). TIY and TEY were normalized to the incident photon flux, recorded as the photocurrent at the photon-flux monitor consisting of a gold-evaporated mesh. All measurements were performed at room temperature.

Figure 13(a) shows AEPICO TOF spectra of PTFE in coincidence with electron emission at a kinetic energy (E_k) of 650 eV upon excitation at photon energies ($h\nu$) of 689.1, 692.6, 696.1, and 720 eV (above F 1s ionization energy). These $h\nu$ are indicated by arrows in figure 13(b) along with the TEY, TIY, and TIY/TEY spectra. In the F 1s near-edge x-ray absorption spectra of PTFE, peaks at $h\nu = 689.1$ and 692.6 eV were assigned to the transitions from F 1s to σ(C–F)* and σ(C–C)* (σ(C–F)* $\leftarrow$ F 1s and σ(C–C)* $\leftarrow$ F 1s), respectively [46]. The appearance of the intense TIY feature at $h\nu = 689.1$ eV, as shown in figure 13(b), indicates that effective ion desorption occurs at σ(C–F)* $\leftarrow$ F 1s. A peak was observed at a TOF difference of about 800 ns in the F 1s AEPICO TOF spectra of PTFE. The intensity of the peak shows a strong $h\nu$ dependence (figure 13(a)). At $h\nu = 689.1$ eV it gives a much higher intensity than those at $h\nu = 692.6$, 691 and 720 eV. This indicates that the ion desorption probability corresponding to the AEPICO peak at the TOF difference of 800 ns at $h\nu = 689.1$ eV is much higher than those at $h\nu = 692.6$, 691 and 720 eV. The AEPICO peak at a TOF difference of about 800 ns could be assigned to F^+.

The AEPICO TOF spectra and an Auger electron spectrum (AES) of PTFE at $h\nu = 689.1$ eV are shown in figure 14. The F^+ AEPICO yield corresponding to the peak intensity at a TOF difference of about 800 ns shows a strong electron E_k dependence. The $h\nu$ and Auger electron E_k dependences of the F^+ AEPICO yield indicate that the effective C–F bond scission of PTFE by core excitation is affected by not only the core electron transition, but also the following Auger transition.

Figures 15(a)–(d) show the electron E_k dependence of the F^+ AEPICO yield (F^+ AEPICO spectra) at $h\nu = 689.1$, 692.6, 691.6 and 720 eV, respectively. For a comparison, the Auger electron spectra (AES) are also shown. In the AES, major, medium and minor peaks appear at E_k of about 650, 630 and 605 eV, respectively. The energy position of the major Auger peak at $h\nu = 689.1$ eV (σ(C–F)* $\leftarrow$ F 1s) is shifted to a higher E_k of about 5 eV, as compared with that at $h\nu = 720$ eV. In general, the kinetic energy of the spectator-Auger electron is larger by a few eV than that of the corresponding normal-Auger electron due to the Coulomb interaction between the Auger electron and the electron excited to the unoccupied state (spectator shift) [47]. Since at $h\nu = 720$ eV (above F 1s ionization energy) the normal-Auger process is mainly considered to occur, the difference AES obtained by subtracting the

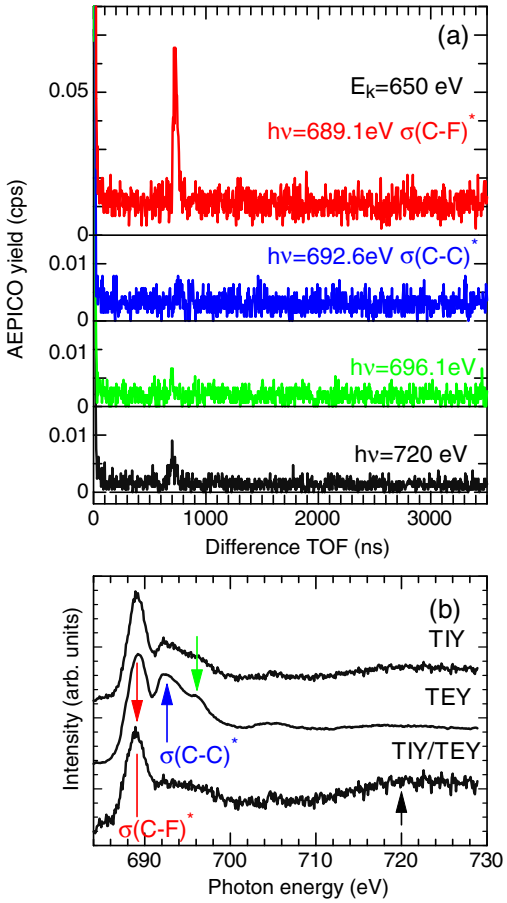

Figure 13. (a) AEPICO TOF spectra of PTFE in coincidence with electron emission at a kinetic energy (E_k) of 650 eV upon excitation at $h\nu = 689.1$, 692.6, 696.1, and 720 eV. (b) Total ion yield (TIY) and total electron yield (TEY) spectra of PTFE for the F K-edge excitation, where the arrows indicate the photon energies used in (a).

Auger spectrum at $h\nu = 720$ eV from resonant AES is expected to provide the spectator- and participator-Auger components in the corresponding resonant AES. This simple procedure has proven to be a convenient approach to extract the spectator-Auger component from a mixture of the spectator- and the normal-Auger processes, because the participator-Auger transitions are reported to be minor processes [48, 49]. An intense peak in the difference AES, obtained by subtracting from the AES at $h\nu = 689.1$ eV, appears at an E_k of 655 eV. It indicates that the main component of the major peak in the Auger spectra at $h\nu = 689.1$ eV is the spectator-Auger electron. In the F KLL AES of fluorides, such as NaF and MgF_2, the AES peaks 652, 630 and 610 eV were assigned to $KL_{23}L_{23}$, KL_1L_{23} and KL_1L_1, respectively [50]. From these, in the AES at $h\nu = 689.1$ eV, the major peak at E_k of 652 eV could be assigned to spectator-Auger final states, where two holes are created in the σ(C–F(2p)) bonding orbitals, and one excited electron remains in the σ(C–F)* antibonding orbital. The AES peak at E_k of 627 eV is also assigned to (valence F(2s))$^{-1}\sigma$(C–F(2p))$^{-1}\sigma$(C–F)*^{1} spectator-Auger final states.

In the AEPICO spectra for the F K-edge excitation shown in figure 15, three peaks appear at E_k of about 650–655, 630, and 610 eV. The intense AEPICO yield is observed at

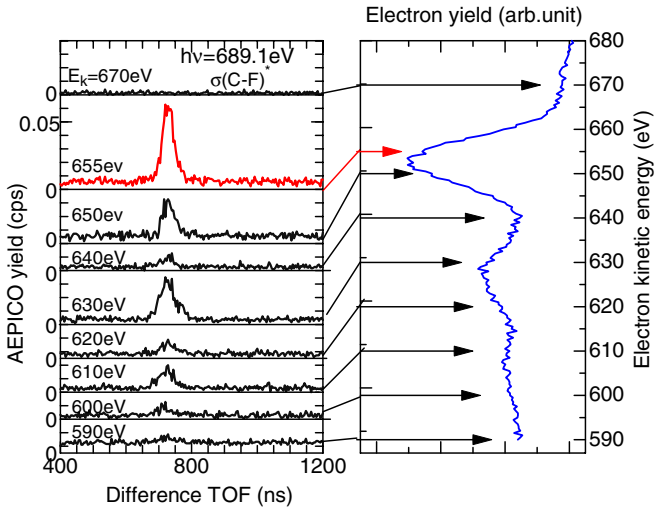

Figure 14. AEPICO TOF spectra (left) and Auger electron spectrum (AES) (right) at $h\nu$ = 689.1 eV for a PTFE thin film. The arrows indicate the E_k employed in measuring the AEPICO TOF spectra.

E_k = 655 eV at σ(C–F)* ← F 1s, as shown in figure 15(a). While the E_k position of this AEPICO intense peak at E_k = 655 eV is shifted to a higher one by about 2 eV than that in the AES, the whole structure of the AEPICO spectrum at $h\nu$ = 689.1 eV is similar to that of the difference AES (spectator component of resonant AES). This indicates that efficient F^+ desorption occurs through spectator-Auger processes at $h\nu$ = 689.1 eV.

The AEPICO yield at $h\nu$ = 692.6 eV corresponding to σ(C–C)* ← F 1s is lower than that at $h\nu$ = 689.1 eV. On the other hand, the whole structure of the difference AES (spectator component of AES) is similar to that of the AEPICO spectrum. This indicates that F^+ desorption at $h\nu$ = 692.6 eV occurs through spectator-Auger decays. At $h\nu$ = 692.6 eV, the spectator shift for the major Auger peak at E_k of about 650 eV is smaller than that upon excitation at $h\nu$ = 689.1 eV. Due to delocalization of the excited electron at the σ(C–C)* antibonding state, the Coulomb interaction between the excited electron and the Auger electron is expected to be smaller. It is considered that delocalization of the excited electron is responsible for suppressing the C–F bond scission. At $h\nu$ = 720 eV (above F 1s ionization energy), normal-Auger processes mainly occur, and the AEPICO spectrum shows a good agreement with the Auger spectrum. This result indicates that a normal-Auger-stimulated ion desorption mechanism is responsible at $h\nu$ above F 1s ionization.

Effective F^+ desorption for PTFE by the irradiation of photons corresponding to σ(C–F)* ← F 1s is attributed to spectator-Auger-stimulated ion desorption. A steep repulsive potential curve of the spectator-Auger final states is expected to be responsible for efficient C–F bond scission. AEPICO spectroscopy combined with synchrotron radiation is a powerful tool to investigate the mechanism of ion desorption induced by core excitation.

6. Ion desorption induced by core excitation of TiO_2(110)

In this section, we show some of the results in which EICO spectroscopy was applied to photostimulated ion desorption (PSID) from a metal oxide surface for investigating its basic mechanism. So far, the Auger-stimulated ion desorption (ASID) mechanism, in which the

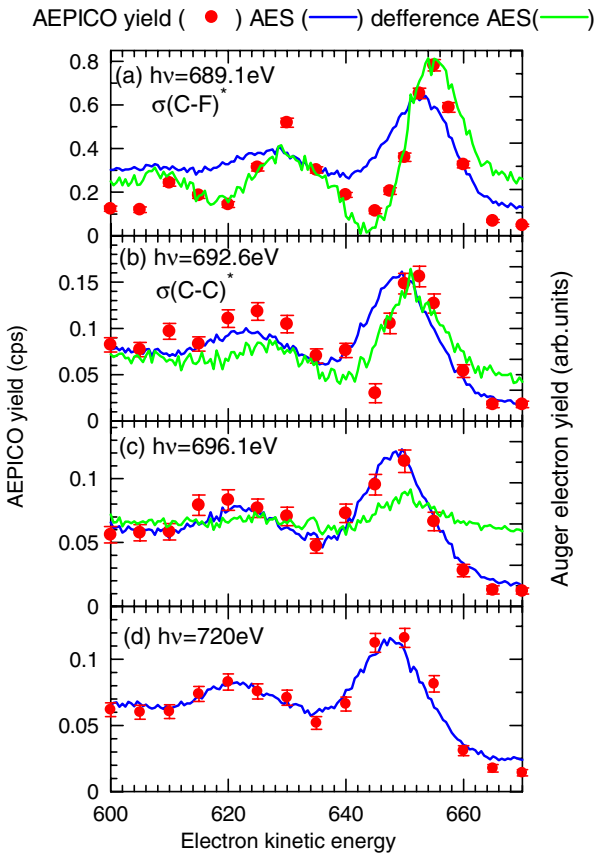

Figure 15. F^+ AEPICO spectra (circles) and Auger electron spectra (AES) (thick solid lines) at $h\nu$ of (a) 689.1, (b) 692.6, (c) 696.1 and (d) 720 eV. The light solid lines in (a)–(c) show the difference AES, which is expected to correspond to the spectator-Auger components.

Coulomb repulsion among valence holes provided by the Auger decay of a core hole is a main driving force for ion desorption, has been accepted as a general model for ion desorption induced by core excitation [6–8]. The ASID mechanism was originally proposed by Knotek and Feibelman for electron-stimulated O^+ desorption from TiO_2. It was based on the results they obtained when measuring the electron-stimulated desorption (ESD) yield of O^+, whose desorption threshold correlates with the Ti 3p core excitation threshold, but not with the O 2s or the valence excitation [13–15]. In the original Knotek–Feibelman (KF) mechanism, proposed for interpreting this experimental result, a Ti 3p core hole is produced by a primary excitation and decays by means of an interatomic Auger process, because there are no higher-lying occupied electronic states, except for the O 2s and O 2p orbitals. (i.e., it is the 'maximal valency' state). This is schematically shown in figure 16(a). In our recent study using EICO spectroscopy on ion desorption from clean and water-adsorbed $TiO_2(110)$ and ZnO(1010) surfaces [51, 52], however, it was shown that the desorption mechanisms following the O 1s excitation and metal-core excitation were different; the former was well described with an ASID model, while the latter could not be fully explained with it.

The lower panels of figure 17 show photoelectron spectra of a clean $TiO_2(110)$ surface taken at $h\nu = 690$ eV (left-hand side) and 190 eV (right-hand side), where the valence bands

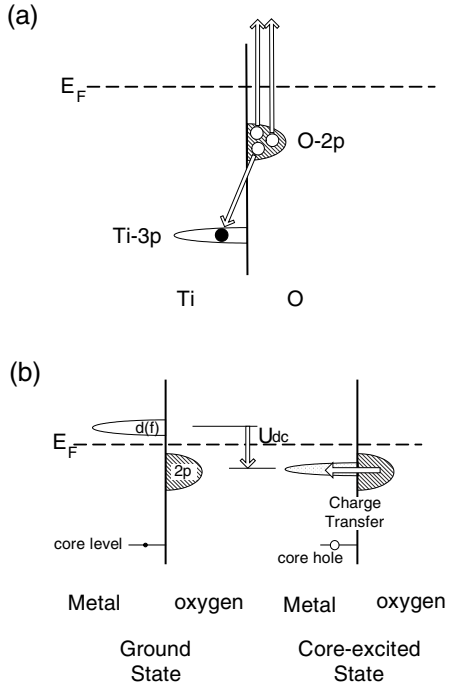

Figure 16. (a) Original Knotek–Feibelman model for TiO_2. Holes at the O 2p level are created by the interatomic Auger decay of a hole at the Ti 3p level. If an additional process, such as a double Auger decay, creates three holes at one oxygen site, O^{2-} is converted into O^+, which is then desorbed because of the repulsive Coulomb force from the surrounding Ti^{4+} ions. E_F here denotes the Fermi energy. (b) Kotani–Toyozawa model for transition metal oxides. When the energy level of the d electrons in the metal site is pulled down by the Coulomb interaction between the core hole and the 3d electrons at the metal site (U_{dc}), charges are transferred from the oxygen p level to the metal d level.

(a), O 2s and 1s ((b), (h)), and Ti 3p, 3s, 2p, and 2s levels ((c), (e), (f), (j)) are observed. The shake-up satellites of Ti 3p (d), Ti 2p (g), O 1s (i), and Ti 2s (k) are also observed. The upper panels of figure 17 show a series of coincidence TOF spectra for desorbed ions and photoelectrons corresponding to the photoelectron peaks (a)–(k). All of the coincidence TOF spectra were normalized so that the background level, which is proportional to the photoelectron intensity, unitys 1. The peaks due to O^+ desorption were observed in the EICO spectra of deeper core levels than Ti 3p, which is in agreement with the electron-energy threshold in the ESD measurement [13]. The relative area intensities of the O^+ peaks can be assumed to be proportional to the O^+ desorption probability per core hole [52]. A comparison among them indicates that the O^+ desorption resulting from the O 1s shake-up excitation is more efficient than that resulting from the O 1s single excitation. In the Ti-core excitation, meanwhile, such enhancements at the satellites are not observed.

This contrast between Ti and O core levels is observed in the O^+ desorption in coincidence with the Auger electron emission from $TiO_2(110)$. The peak-area intensities of photostimulated O^+ from $TiO_2(110)$ in the EICO TOF spectra as a function of the electron energy and their errors derived from the standard deviation of the backgrounds are shown in figure 18 together with the AES. In the case of the Ti-related Auger electron emission (shown in the left part of the figure), the peaks in the normalized O^+ yield are at energies similar to those of the peaks

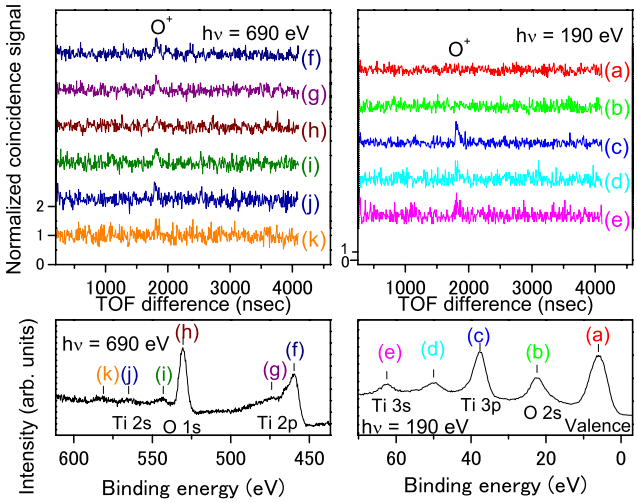

Figure 17. The lower panels show the photoelectron spectra of a clean $TiO_2(110)$ surface taken at $h\nu = 690$ eV (left-hand side) and 190 eV (right-hand side), where (a) the valence bands, (b) O 2s, (c) Ti 3p, (d) shake-up satellites of Ti 3p, (e) Ti 3s, (f) Ti 2p, (g) shake-up satellites of Ti 2p, (h) O 1s, (i) shake-up satellites of O 1s, (j) Ti 2s, and (k) shake-up satellites of Ti 2s appears. The upper panels show a series of coincidence TOF spectra for desorbed ions and photoelectrons corresponding to the photoelectron peaks (a)–(k).

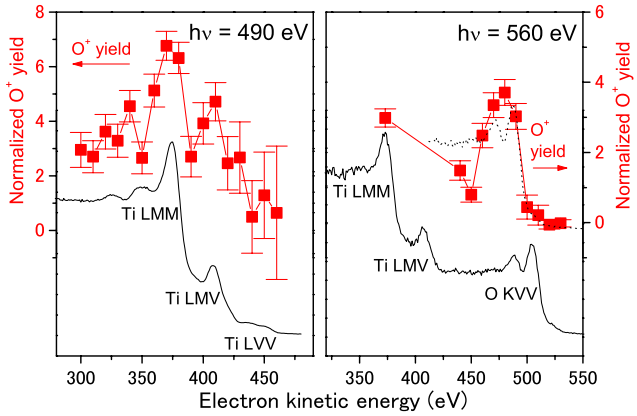

Figure 18. Peak-area intensities of photostimulated O^+ from $TiO_2(110)$ in the EICO TOF spectra as a function of the electron energy and their errors derived from the standard deviation of the backgrounds together with the AES of $TiO_2(110)$.

in the AES. In the O-related Auger emission, in contrast, the peak in the normalized O^+ yield is not at the energy of the O KVV Auger electrons, but is shifted to a lower energy. The dotted line in the right-hand panel shows the AES shifted by −17 eV (approximate to the shake-up energy) and is, except for the increased width of the O^+ yield peak, in agreement with the O^+ yield. Furthermore, as in the case of the O^+ desorption from the clean $TiO_2(110)$ surface, the H^+ peaks for both water-adsorbed $TiO_2(110)$ and ZnO(1010) reach their maximum intensity not at the O-Auger main peak, but on its lower-kinetic-energy side.

These results indicate that ion desorption induced by O 1s excitations on the $TiO_2(110)$ and Zn(1010) surfaces is not practically due to the two-hole final state resulting from a

normal Auger decay, but mainly to the three-hole final state resulting from multi-electron excitation/decay. In the case of the O^+ desorption from $TiO_2(110)$, this result is related to the fact that oxygen in TiO_2 is nominally O^{2-}, so the desorption of O^+ would require three electrons to be removed from the oxygen atoms, and this mechanism is similar to that proposed by KF [13–15]. Ion desorption due to multi-electron excitation/decay was also clearly observed for that on a water-adsorbed Si(100) surface by using the EICO technique [28], as well as H_2O/Si(111) and H_2O/SiO_2/Si(111), as described in section 3. The mechanism of ion desorption due to the Ti-core excitations, however, seems not to be similar to the case of the O-core excitations. If a simple formulation is assumed for the core excitation and Auger decay process, the observed results indicate that the two-hole final state, which is provided by the single-electronic excitation and its normal Auger decay, yields an efficiency of O^+ desorption, similar to the case of the n-hole ($n > 2$) final state. This is contradictory to the fact that at least three charges are necessary to transfer for converting O^{2-} to O^+. Furthermore, a 'maximal valency' criterion, which was originally proposed to account for the ion desorption from metal oxide, in fact does not work in many systems investigated after the original KF work. A new criterion, in which ion desorption associated with metal-core excitation occurs when the metals are light d and f metals, such as Ti, V, W, Cr, La, Ce, Nb, and Er [52], is more appropriate.

According to studies of photoelectron spectroscopy, the core-hole potential at the metal site pulls down the energy of the d and f levels, in the final state of the core-level photoemission of the d- and f-transition-metal oxide, enabling charge to be transferred from the O 2p orbital to the metal through their hybridization, as shown in figure 16(b). This is the 'Kotani–Toyozawa' mechanism, and is well established in the field of photoelectron spectroscopy [53]. This mechanism of charge transfer from the O 2p orbital to the Ti 3d orbital, instead of the interatomic Auger transition, was proposed to be the force driving O^+ desorption from $TiO_2(110)$ surfaces [52]. Since the final state of the main peak as well as the satellite peak of Ti-related photoexcitation is due to a mixture of several electronic configurations, a simple explanation, such as one that the main peak in the photoelectron spectrum corresponds to the single-electron excitation and the satellite peak corresponds to the two-electron excitation, which was valid with regard to the O 1s excitation, is not applicable to the excitation/decay of the Ti core level. This is consistent with our EICO results. Furthermore, this mechanism satisfies the new criterion. The charge transfer is dominated by effective hybridization between the O 2p and metal d (f) orbitals ($V_{\mathrm{eff}} = \sqrt{n_{\mathrm{h}}}V$, where n_{h} is the formal number of the d (f) holes in the ground state and V is the hybridization) in the Kotani–Toyozawa model. This value is larger for the metal oxide from which the metal-core-induced ion desorption occurs. This model also predicts that metal-core-excitation-induced ion desorption would not occur from non-transition-metal compounds, which is consistent with the previous experimental results and an EICO study on a water-adsorbed Zn(1010) surface [52]. In any case, the model described here explains only the process of the charge transfer, which is the very first process of ion desorption. We have to note that the charge transfer from oxygen to metal is somewhat delocalized in the new model, and there must be a process localizing these holes into one oxygen atom before ion desorption. More work will be necessary to understand the details of ion desorption from metal compounds.

7. Conclusion and future prospects

In this paper we have described recent photostimulated ion desorption (PSID) studies using EICO spectroscopy. For H_2O/Si(111) and H_2O/SiO_2/Si(111), the H^+ desorption probabilities per Si 2p ionization were quantitatively estimated. We proposed a mechanism that H^+ desorption is induced by Si 2p photoionization accompanied by a Si LVVV double-Auger

transition. This article also reviews recent EICO work on site-specific ion desorption of $CF_3CD(OH)CH_3$ adsorbed on Si(100), and on the mechanisms of PSID from PTFE and $TiO_2(110)$. Clear site-specific ion desorption was observed for the C 1s core excitation of a $CF_3CD(OH)CH_3$ sub-monolayer on Si(100). A spectator-Auger-stimulated ion desorption mechanism was proposed for F^+ desorption from PTFE at $\sigma(\text{C–F})^* \leftarrow$ F 1s. O^+ desorption induced by O 1s excitation of $TiO_2(110)$ was attributed mainly to three-hole final states resulting from multi-electron excitation/decay. For O^+ desorption induced by Ti core excitation of $TiO_2(110)$, on the other hand, charge transfer from an O 2p orbital to a Ti 3d orbital, instead of an interatomic Auger transition, was proposed to be responsible for the desorption. These investigations demonstrate that EICO spectroscopy combined with synchrotron radiation is a useful tool for studying PSID.

Although EICO spectroscopy has developed into a powerful and convenient tool for PSID studies, there is still room for improvement. The electron-energy resolution, the ion-mass resolution and the signal-to-background ratio will be improved if the electrodes of the EICO analyser are optimized. The coincidence measurements between an electron and an energy-selected ion will offer information on the potential energy surface responsible for PSID. Coincidence between an electron and an angle-resolved ion will clarify the configuration of surface molecules at a specific site. For desorption studies of excited neutrals the coincidence between an electron and excited neutrals is promising. EICO spectroscopy combined with vacuum ultraviolet light, hard x-rays, γ-rays, electron beams, ion beams, multiply charged ion beams, energetic neutral beams, metastable atom beams and positron beams are also prospective fields. EICO spectroscopy also has a potential as a surface analysis technique.

Acknowledgments

We are grateful to Professor Nobuo Ueno (Chiba University) for fruitful discussions. This work was partly supported by Grants-in-Aid for Scientific Research 14540314 and 16560021, and the 21st Century COE Program ‘Frontiers of super-functionality organic devices’ from the Japanese Ministry of Education, Culture, Sports, Science and Technology. This work was performed under approval of the Photon Factory Program Advisory Committee (PF PAC No 2002G103, 2004G026).

References

[1] Isikawa Y 1942 *Rev. Phys. Chem. Japan* **16** 83 (in Japanese)
Isikawa Y 1942 *Rev. Phys. Chem. Japan* **16** 117 (in Japanese)
Isikawa Y 1942 *Proc. Imp. Acad. (Tokyo)* **18** 246
Isikawa Y 1942 *Proc. Imp. Acad. (Tokyo)* **18** 390
[2] Isikawa Y 1943 *Rev. Phys. Chem. Japan* **17** 176 (in Japanese)
Isikawa Y 1943 *Rev. Phys. Chem. Japan* **17** 190 (in Japanese)
Isikawa Y 1943 *Proc. Imp. Acad. (Tokyo)* **19** 380
Isikawa Y 1943 *Proc. Imp. Acad. (Tokyo)* **19** 385
[3] Ohta Y 1943 *J. Chem. Soc. Japan* **64** 849 (in Japanese)
Ohta Y 1943 *J. Chem. Soc. Japan* **64** 986 (in Japanese)
Ohta Y 1943 *J. Chem. Soc. Japan* **64** 1045 (in Japanese)
Ohta Y 1960 *Oyo Buturi* **29** 826 (in Japanese)
Ohta Y 1960 *Oyo Buturi* **29** 834 (in Japanese)
[4] Menzel D and Gomer R 1964 *J. Chem. Phys.* **40** 1164
Menzel D and Gomer R 1964 *J. Chem. Phys.* **41** 3311
Menzel D and Gomer R 1964 *J. Chem. Phys.* **41** 3329
[5] Redhead P A 1964 *Can. J. Phys.* **42** 886
[6] Ramsier R D and Yates J T Jr 1991 *Surf. Sci. Rep.* **12** 246

[7] Madey T E 1994 *Surf. Sci.* **299/300** 824
[8] Feulner P and Menzel D 1995 *Laser Spectroscopy and Photochemistry on Metal Surfaces* ed H L Dai and W Ho (Singapore: World Scientific) p 627
[9] Feulner P, Romberg R, Frigo S P, Weimar R, Gsell M, Ogurtsov A and Menzel D 2000 *Surf. Sci.* **451** 41
[10] Mase K, Nagasono M, Tanaka S, Sekitani T and Nagaoka S 2003 *Fiz. Nizk. Temp.* **29** 321
Mase K, Nagasono M, Tanaka S, Sekitani T and Nagaoka S 2003 *Low Temp. Phys.* **29** 243 (Engl. Transl.)
[11] Baba Y 2003 *Fiz. Nizk. Temp.* **29** 303
Baba Y 2003 *Low Temp. Phys.* **29** 228 (Engl. Transl.)
[12] Jaeger R, Stöhr J and Kendelewicz T 1983 *Phys. Rev.* B **28** 1145
[13] Knotek M L and Feibelman P J 1978 *Phys. Rev. Lett.* **40** 964
[14] Feibelman P J and Knotek M L 1978 *Phys. Rev.* B **18** 6531
[15] Knotek M L and Feibelman P J 1979 *Surf. Sci.* **90** 78
[16] Franchy R and Menzel D 1979 *Phys. Rev. Lett.* **43** 865
[17] Haak H W, Sawatzky G A and Thomas T D 1978 *Phys. Rev. Lett.* **41** 1825
[18] Barakdar J and Kirschner J (ed) 2004 *Correlation Spectroscopy of Surfaces, Thin Films and Nanostructures* (Weinheim: Wiley–VCH)
[19] Mase K, Nagasono M, Tanaka S, Urisu T and Nagaoka S 1997 *Surf. Sci.* **377–379** 376
[20] Mase K, Nagasono M, Tanaka S, Kamada M, Urisu T and Murata Y 1997 *Rev. Sci. Instrum.* **68** 1703
[21] Tanaka K, Sako E O, Ikenaga E, Isari K, Sardar S A, Wada S, Sekitani T, Mase K and Ueno N 2001 *J. Electron Spectrosc. Relat. Phenom.* **119** 255
[22] Mase K, Tanaka S, Nagaoka S and Urisu T 2000 *Surf. Sci.* **451** 143
[23] Mase K, Nagasono M and Tanaka S 1999 *J. Electron Spectrosc. Relat. Phenom.* **101–103** 13
[24] Siegbahn K, Kholine N and Golikov G 1997 *Nucl. Instrum. Methods Phys. Res.* A **384** 563
[25] Isari K, Yoshida H, Gejo T, Kobayashi E, Mase K, Nagaoka S and Tanaka K 2003 *J. Vac. Soc. Japan* **46** 377 (in Japanese)
[26] Kobayashi E, Isari K and Mase K 2003 *Surf. Sci.* **528** 255
[27] Sekiguchi T, Ikeura H, Tanaka K, Obi K, Ueno N and Honma K 1995 *J. Chem. Phys.* **102** 1422
[28] Tanaka S, Mase K, Nagaoka S, Nagasono M and Kamada M 2002 *J. Chem. Phys.* **117** 4479
[29] Hollinger G and Himpsel F J 1983 *J. Vac. Sci. Technol.* A **1** 640
[30] Eberhardt W, Sham T K, Carr R, Krummacher S, Strongin M, Weng S L and Wesner D 1983 *Phys. Rev. Lett.* **50** 1038
[31] Müller-Dethlefs K, Sander M, Chewter L A and Schlag E W 1984 *J. Phys. Chem.* **88** 6098
[32] Hanson D M 1990 *Adv. Chem. Phys.* **77** 1
[33] Tinone M C K, Tanaka K, Maruyama J, Ueno N, Imamura M and Matsubayashi N 1994 *J. Chem. Phys.* **100** 5988
[34] Nenner I, Reynaud C, Schmelz H C, Ferrand-Tanaka L, Simon M and Morin P 1996 *Z. Phys. Chem.* **195** 43
[35] Romberg R, Heckmair N, Frigo S P, Ogurtsov A, Menzel D and Feulner P 2000 *Phys. Rev. Lett.* **84** 374
[36] Nagaoka S, Tamenori Y, Hino M, Kakiuchi T, Ohshita J, Okada K, Ibuki T and Suzuki I H 2005 *Chem. Phys. Lett.* **412** 459 and references cited therein
[37] Nagaoka S, Mase K, Nakamura A, Nagao M, Yoshinobu J and Tanaka S 2002 *J. Chem. Phys.* **117** 3961
[38] Nagaoka S, Mase K, Nagasono M, Tanaka S, Urisu T, Ohshita J and Nagashima U 1999 *Chem. Phys.* **249** 15
[39] Nagaoka S, Tanaka S and Mase K 2001 *J. Phys. Chem.* B **105** 1554
[40] Womack M, Vendan M and Molian P 2004 *Appl. Surf. Sci.* **221** 99
[41] Wheeler D R and Pepper S V 1982 *J. Vac. Sci. Technol.* **20** 442
[42] Clark D T and Brennan W J 1986 *J. Electron Spectrosc. Relat. Phenom.* **41** 399
[43] Okudaira K K, Yamane H, Ito K, Imamura M, Hasegawa S and Ueno N 2002 *Surf. Rev. Lett.* **9** 335
[44] Okudaira K K, Setoyama H, Yagi H, Mase K, Kera S, Kahn A and Ueno N 2004 *J. Electron Spectrosc. Relat. Phenom.* **137–140** 137
[45] Kobayashi E, Isari K, Mori M, Nambu A and Mase K 2004 *J. Vac. Soc. Japan* **47** 14 (in Japanese)
[46] Ohta T, Seki K, Yokoyama T, Morisada I and Edamatsu K 1990 *Phys. Scr.* **41** 152
[47] Sasaki T A, Baba Y, Yoshii K and Yamamoto H 1995 *J. Phys.: Condens. Matter* **7** 463
[48] Aksela H, Aksela S, Mantykentta A, Tulkki J, Shigemasa E, Yagishita A and Furusawa Y 1992 *Phys. Scr.* T **41** 113
[49] Mase K, Nagasono M, Tanaka S, Urisu T, Ikenaga E, Sekitani T and Tanaka K 1997 *Surf. Sci.* **390** 97
[50] Kövér L, Uda M, Cserny I, Tóth J, Végh J, Varga D, Ogasawara K and Adachi H 2001 *J. Vac. Sci. Technol.* A **19** 1143
[51] Tanaka S, Mase K, Nagasono M, Nagaoka S and Kamada M 2000 *Surf. Sci.* **451** 182
[52] Tanaka S, Mase K and Nagaoka S 2004 *Surf. Sci.* **572** 43 and references therein
[53] Hüfner S 2003 *Photoelectron Spectroscopy* 3rd edn (Berlin: Springer) p 114